Solving time-dependent problems by an RBF-PS method with an optimal shape parameter

2009 J. Phys.: Conf. Ser. 181 012053

(http://iopscience.iop.org/1742-6596/181/1/012053)

Journal of Physics: Conference Series **181** (2009) 012053 doi:10.1088/1742-6596/181/1/012053

Solving time-dependent problems by an RBF-PS method with an optimal shape parameter

Ana M. A. Neves[1], C. M. C. Roque[1], A. J. M. Ferreira[1], C. M. M. Soares[2], R. M. N. Jorge[1]

[1] Departamento de Engenharia Mecânica e Gestão Industrial, Faculdade de Engenharia da Universidade do Porto,
Rua Dr. Roberto Frias, 4200-465 Porto, Portugal
[2] IDMEC - Instituto de Engenharia Mecânica - Instituto Superior Técnico, Av. Rovisco Pais, 1096 Lisboa Codex, Portugal

E-mail: ana.m.neves@fe.up.pt,croque@fe.up.pt,ferreira@fe.up.pt, cristovao.mota.soares@dem.ist.utl.pt,rnatal@fe.up.pt

Abstract. An hybrid technique is used for the solutions of static and time-dependent problems. The idea is to combine the radial basis function (RBF) collocation method and the pseudospectal (PS) method getting to the RBF-PS method. The approach presented in this paper includes a shape parameter optimization and produces highly accurate results.

Different examples of the procedure are presented and different radial basis functions are used. One and two-dimensional problems are considered with various boundary and initial conditions. We consider generic problems, but also results on beams and plates. The displacement and the stress analysis are conducted for static and transient dynamic situations. Results obtained are in good agreement with exact solutions or references considered.

1. Introduction

Both pseudospectral (PS) method ([1, 2]) and radial basis function (RBF) method ([3] to [7]) are good solvers for PDEs. Combining the two methods we can extend the high accuracy of the results to complex geometries and keep it simple to implement.

Ferreira and colleagues used the multiquadrics RBF ([8]) to solve time-dependent problems including structural problems. Fasshauer, Ferreira, and colleagues ([9] to [14]) have already used with success the RBF-PS method for the solution of some problems. This paper extends the application of the RBF-PS method to the transient analysis of structural problems including an optimization of the shape parameter for the radial basis functions, allowing an user-independent analysis.

2. RBF-PS method for time-dependent problems

Suppose you want to approximate a function that you want to differentiate or to approximate the solution $u(x)$ or $u(x,t)$ of a given a differential equation with boundary conditions. The approximation considered is a finite sum of very smooth and global basis functions,

$$u(x) = \sum_{k=0}^{N} \lambda_k \phi_k(x), \text{ in the case of static problems} \tag{1}$$

$$\text{or} \quad u(x,t) = \sum_{k=0}^{N} \lambda_k(t)\phi_k(x), \text{ for time-dependent problems} \tag{2}$$

where the basis functions $\phi_k(x)$ can be for example trigonometric functions or polynomials, such as Chebyshev polynomials. Then, you differentiate these functions exactly ([2]).

When using pseudospectral method, if you are given a set of grid points x_i and corresponding function values $u_i = u(x_i)$, you can use this data to approximate the derivative of u via *differentiation matrices*. Writing u as a column vector, you can find a square matrix D such that, at x_i, you have

$$u' = D.u. \tag{3}$$

Finding the derivative of a vector of data becomes a $matrix \times vector$ multiplication. We just need some manipulations to get to D.

You must evaluate (1) at the grid points x_i and get

$$u(x_i) = \sum_{k=0}^{N} \lambda_k \phi_k(x_i), \tag{4}$$

or in matrix-vector notation

$$u = A\lambda, \tag{5}$$

where λ is the column vector of the coefficients λ_k, matrix A has entries $A_{ik} = \phi_k(x_i)$, and u is as before. If you ensure that A is invertible, you get

$$\lambda = A^{-1}.u. \tag{6}$$

Recall that the invertibility of matrix A depends both on the basis function chosen and the location of the points x_i. For univariate polynomials with a set of distinct points invertibility is ensured.

On the other hand, differentiating both sides of (1), you get

$$\frac{d}{dx}u(x) = \sum_{k=1}^{N} \lambda_k \frac{d}{dx}\phi_k(x) \tag{7}$$

Evaluating at the grid points x_i we get in matrix-vector notation

$$u' = M\lambda, \tag{8}$$

where λ is the column vector of the coefficients λ_k, matrix M has entries $M_{ik} = \frac{d}{dx}\phi_k(x_i)$, and u is as before.

So, using (6) in (8), we obtain $u' = M.A^{-1}.u$ so that the differentiation matrix D we were looking for in (3) is

$$D = M.A^{-1}. \tag{9}$$

D_{ij} is the derivative of the j^{th} curve at x_i.

In this paper we use (infinitely smooth) radial basis functions in a spectral framework. The basis function expansion $\phi_k(x)$ in (1) will take the form $\phi_k(x) = g(||x - x_k||, \epsilon) = g(r, \epsilon)$, chosen from a list more extense than the following ([14] among others), e.g.:

$$g(r,\epsilon) = e^{-(\epsilon r)^2}; \qquad \text{gaussian} \tag{10}$$

$$g(r,\epsilon) = 1/\sqrt{(1+(\epsilon r)^2)}; \qquad \text{inverse multiquadric} \tag{11}$$

$$g(r,\epsilon) = e^{-\epsilon r}(15 + 15\epsilon r + 6(\epsilon r)^2 + (\epsilon r)^3); \qquad \text{cubic matérn} \tag{12}$$

$$g(r,\epsilon) = \sqrt{1+(\epsilon r)^2}; \qquad \text{multiquadric} \tag{13}$$

$$g(r,\epsilon) = max(1-\epsilon r, 0)^8(32(\epsilon r)^3 + 25(\epsilon r)^2 + 8\epsilon r + 1) \qquad \text{Wendland's } \varphi_{3,3} \tag{14}$$

being r the (Euclidean) distance and ϵ a free parameter.

For the RBF-PS technique, matrix A in (5) and (9) has entries

$$A_{ij} = g(r_j, \epsilon)_{|x=x_i} = g(||x_i - x_j||, \epsilon). \tag{15}$$

Furthermore, the entries of M in (8) become $\frac{d}{dx} g(r, \epsilon)_{|x=x_i}$.

In all dynamic problems, depending on the nature of the problem, at each time t we can approximate $u(x,t)$ or $u(x,y,t)$ considering the *forward Euler method* or the *leap frog method*, for example:

$$\frac{\partial u}{\partial t} \approx \frac{u(x, t_{n+1}) - u(x, t_n)}{\Delta t} \tag{16}$$

$$\frac{\partial u}{\partial t} \approx \frac{u(x, t_{n+1}) - u(x, t_{n-1})}{2\Delta t} \tag{17}$$

$$\frac{\partial^2 u}{\partial t^2} = \frac{\partial}{\partial t}\left(\frac{\partial u}{\partial t}\right) \approx \frac{u(x, t_{n+1}) - 2u(x, t_n) + u(x, t_{n-1})}{(\Delta t)^2} \tag{18}$$

being $\Delta t = t_{n+1} - t_n$. This allows us to march in time. The key to the solution of the problems is the approximation of the spatial derivative, both in dynamic or static problems.

To solve a PDE like

$$\frac{\partial}{\partial t} u(x,t) + \frac{\partial}{\partial x} u(x,t) = 0 \tag{19}$$

using the rbf-spectral differentiation matrix D to express the spatial derivative and (16) leads to

$$u(x, t_{n+1}) = u(x, t_n) - \Delta t . D . u(x, t_n) \tag{20}$$

The procedure just described can be generalized to more complex linear differential operators. In this paper we are interested in those such as the ones involved in the following PDE's

$$\frac{\partial}{\partial t} u(x,t) = \frac{\partial^2}{\partial x^2} u(x,t) \tag{21}$$

$$\frac{\partial^2}{\partial t^2} u(x,t) = \frac{\partial^2}{\partial x^2} u(x,t) \tag{22}$$

If we use (16) for the time derivative and the second order rbf-spectral differential matrix D^2 for the spatial derivative, (21) leads to

$$u(x, t_{n+1}) = u(x, t_n) + \Delta t . D^2 . u(x, t_n) \tag{23}$$

and if we use (18) for the time derivative and the second order rbf-spectral differential matrix D^2 for the spatial derivative, (22) leads to

$$u(x, t_{n+1}) = 2 * u(x, t_n) - u(x, t_{n-1}) + (\Delta t)^2 * D^2 * u(x, t_n); \tag{24}$$

where D^2 is defined as $D^2 = M^2 . A^{-1}$ being $M^2_{ik} = \frac{d^2}{dx^2} g(||x_i - x_k||, \epsilon)$.

In general, D^p_{ij} is the p^{th} derivative of curve number j at x_i:

$$D^p = M^p . A^{-1} \tag{25}$$

being $M^p_{ik} = \frac{d^p}{dx^p} g(||x_i - x_k||, \epsilon)$.

Table 1. Solution errors (%) for problem 3.1.1 with 11 Chebyshev points, $\Delta t = 0.001$, and Wendland C6 RBF

time	$E_{x_0=1}$	E_{x_1}	E_{x_2}	E_{x_3}	E_{x_4}	E_{x_5}
0.1	1.169e-1	1.167e-1	1.125e-1	9.735e-2	6.853e-2	3.477e-2
0.2	8.727e-2	8.716e-2	8.505e-2	7.722e-2	6.102e-2	3.898e-2
0.3	6.484e-2	6.478e-2	6.369e-2	5.959e-2	5.102e-2	3.909e-2
0.4	5.170e-2	5.166e-2	5.113e-2	4.914e-2	4.496e-2	3.913e-2
0.5	4.498e-2	4.496e-2	4.472e-2	4.379e-2	4.185e-2	3.917e-2

For the solution of a two-dimensional problem involving $\frac{\partial}{\partial x}u(x,y,t)$, $\frac{\partial}{\partial y}u(x,y,t)$, $\frac{\partial^2}{\partial x^2}u(x,y,t)$, $\frac{\partial^2}{\partial x \partial y}u(x,y,t)$, or $\frac{\partial^2}{\partial y^2}u(x,y,t)$ we can use the same approximation of the time derivative but we must use different differentiation matrix for the approximation of each spatial derivative. We consider the following approximations, e.g.:

$$\frac{\partial}{\partial x}u(x,y,t) \approx D_x.u(x,y,t) \qquad D_x = \frac{\partial}{\partial x}g(r,\epsilon)_{|(x,y)=(x_i,y_i)}.A^{-1} \tag{26}$$

$$\frac{\partial^2}{\partial x^2}u(x,y,t) \approx D_{xx}.u(x,y,t) \qquad D_{xx} = \frac{\partial^2}{\partial x^2}g(r,\epsilon)_{|(x,y)=(x_i,y_i)}.A^{-1} \tag{27}$$

$$\frac{\partial^2}{\partial x \partial y}u(x,y,t) \approx D_{xy}.u(x,y,t) \qquad D_{xy} = \frac{\partial^2}{\partial x \partial y}g(r,\epsilon)_{|(x,y)=(x_i,y_i)}.A^{-1} \tag{28}$$

$$\tag{29}$$

being $g(r,\epsilon)$ the chosen RBF and A as in (15).

The question of the invertibility of the matrix A remains unsolved for some cases. Fasshauer presents detailed information on the subject in his book [14].

The optimization of the RBF shape parameter is the same used in [12, 13, 14] and a fairly detailed exposition is available in these references.

3. Numerical examples

3.1. One-dimensional problems

3.1.1. Initial-boundary-value problem 1

$$\begin{cases} \text{PDE} & \frac{\partial u}{\partial t} = \frac{\partial^2 u}{\partial x^2},\ 0 \le x \le 1,\ t \ge 0 \\ \text{BC} & \frac{\partial u}{\partial x}(0,t) = \frac{\partial u}{\partial x}(1,t) = 0,\ t \ge 0 \\ \text{IC} & u(x,0) = 9 + 3\cos(\pi x) + 5\cos(4\pi x),\ 0 \le x \le 1 \end{cases} \tag{30}$$

The PDE was implemented for the RBF-PS method as $u_{t+1} = u_t + \Delta t.D2.u_t$.

In tables 1-2 we present the results obtained with present method. We compare with the exact solution $u(x,t) = 9 + 3e^{-\pi^2 t}\cos(\pi x) + 5e^{-16\pi^2 t}\cos(4\pi x)$. Results are in good agreement, the biggest error being approximately 0.2%.

Using 11 Chebyshev points, $\Delta t = 0.001$, and Wendland C6 RBF, the optimized shape parameter is $\epsilon = 0.100064$. For the same RBF but using 21 Chebyshev points and $\Delta t = 0.0001$, we get $\epsilon = 0.160453$. If we use 11 Chebyshev points, $\Delta t = 0.001$, and the Matérn Cubic RBF, we obtain $\epsilon = 0.276603$. Using 21 Chebyshev points, the Matérn Cubic RBF, and $\Delta t = 0.0001$, we get $\epsilon = 1.250831$.

Using 21 Chebyshev points the error achieves a value smaller than $5 * 10^{-5}$%.

Table 2. Solution errors (%) for problem 3.1.1 with 11 Chebyshev points, $\Delta t = 0.001$, and Matérn Cubic RBF

time	$E_{x_0=1}$	E_{x_1}	E_{x_2}	E_{x_3}	E_{x_4}	E_{x_5}
0.1	1.175e-1	1.173e-1	1.132e-1	9.823e-2	6.971e-2	3.611e-2
0.2	8.809e-2	8.800e-2	8.594e-2	7.824e-2	6.225e-2	4.038e-2
0.3	6.590e-2	6.584e-2	6.477e-2	6.075e-2	5.229e-2	4.046e-2
0.4	5.286e-2	5.283e-2	5.231e-2	5.036e-2	4.625e-2	4.046e-2
0.5	4.618e-2	4.617e-2	4.593e-2	4.503e-2	4.313e-2	4.046e-2

3.1.2. Initial-boundary-value problem 2

$$\begin{cases} \text{PDE} & \frac{\partial^2 u}{\partial t^2} = \frac{\partial^2 u}{\partial x^2},\ 0 \le x \le \pi,\ t \ge 0 \\ \text{BC} & u(0,t) = u(\pi,t) = 0,\ t \ge 0 \\ \text{IC} & \begin{cases} u(x,0) = \pi x - x^2,\ 0 \le x \le \pi \\ \frac{\partial u}{\partial t}(x,0) = 0,\ 0 \le x \le \pi \end{cases} \end{cases} \tag{31}$$

To solve this problem we considered $\Delta t = 1.5625 * 10^{-5}$ and 81 Chebyshev points for $t \in [0, 4]$. Results obtained with the RBF-PS method, with an optimized shape parameter, both for Matérn Cubic and Wendland C6 RBF are in good agreement with the exact solution, which is $u(x,t) = \frac{8}{\pi} \sum_{odd\ n} n^{-3} \sin(nx)\cos(nt)$. The error is lower than 1% except for the boundary as the exact solution here is equal to zero for every t and around $t = 1.6$ which corresponds to values near zero for the exact solution.

The values for the shape parameter are quite different as we change the RBF: for the Matérn Cubic RBF the optimal shape parameter obtained was $\epsilon = 4.142739$ and for the Wendland C6 was $\epsilon = 0.962844$.

3.1.3. Transient analysis of a beam For the transient dynamic study of a beam in bending we are using the first-order shear deformation theory (FSDT) ([15]), with shear correction factor $K = 5/6$. When applied to beams, the equations of motion are

$$KGbh\left(\frac{\partial^2 w_0}{\partial x^2} + \frac{\partial \theta_x}{\partial x}\right) + bq = bI_0 \frac{\partial^2 w_0}{\partial t^2} \tag{32}$$

$$EI\frac{\partial^2 \theta_x}{\partial x^2} - KGbh\left(\frac{\partial w_0}{\partial x} + \theta_x\right) = bI_2 \frac{\partial^2 \theta_x}{\partial t^2} \tag{33}$$

Here, $w = w(x,t)$ is the transverse displacement, $\theta_x = \theta_x(x,t)$ is the rotation about the x axis, $K = 5/6$ is the shear correction coefficient, and q is the total transverse load. The remaining terms are obtained from given constants that characterize both the material properties and the structural properties of the beam.

We use the static solution of bending equilibrium as the initial conditions.

For the time-steping procedure we considered equations (32) and (33) divided by bI_0 and bI_2, respectively, and used the *forward Euler method*.

We consider an isotropic beam with both ends simply-supported and material properties $E = 10920;\ \rho = 1;\ \nu = 0.25$. The dimensions of the beam are $a = 1,\ b = 1,\ h = 0.1$, being a the length, h the thickness, and $b * h$ the cross section dimensions.

We used 11 Chebyshev points along the beam, $x \in [0, 1]$, the Cubic Matérn RBF (see (12)), and $\Delta t = 5 * 10^{-5}$. The optimal RBF shape parameter obtained was $\epsilon = 0.276603$.

In figure 1 we present the transverse displacement of the central point of the beam for $t \in [0, 1]$.

3.2. Transient analysis of a plate

Consider now an isotropic square plate in bending, clamped at all edges. Length of each side is $a = 2$ and side-over-thickness ratio is $a/h = 10$. The material properties are $\rho = 1$, $E = 10920$, and $\nu = 0.3$.

In the present study the First-Order Shear Deformation Theory (FSDT) is used ([15]). When applied to plates, the equations of motion are

$$D_{11}\frac{\partial^2\theta_x}{\partial x^2} + D_{16}\frac{\partial^2\theta_y}{\partial x^2} + (D_{12}+D_{66})\frac{\partial^2\theta_y}{\partial x\partial y} + 2D_{16}\frac{\partial^2\theta_x}{\partial x\partial y} + D_{66}\frac{\partial^2\theta_x}{\partial y^2} + D_{26}\frac{\partial^2\theta_y}{\partial y^2} + \\ - kA_{45}\left(\theta_y + \frac{\partial w}{\partial y}\right) - kA_{55}\left(\theta_x + \frac{\partial w}{\partial x}\right) = I_2\frac{\partial^2\theta_x}{\partial t^2} \quad (34)$$

$$D_{16}\frac{\partial^2\theta_x}{\partial x^2} + D_{66}\frac{\partial^2\theta_y}{\partial x^2} + (D_{12}+D_{66})\frac{\partial^2\theta_x}{\partial x\partial y} + 2D_{26}\frac{\partial^2\theta_y}{\partial x\partial y} + D_{26}\frac{\partial^2\theta_x}{\partial y^2} + D_{22}\frac{\partial^2\theta_y}{\partial y^2} + \\ - kA_{44}\left(\theta_y + \frac{\partial w}{\partial y}\right) - kA_{45}\left(\theta_x + \frac{\partial w}{\partial x}\right) = I_2\frac{\partial^2\theta_y}{\partial t^2} \quad (35)$$

$$\frac{\partial}{\partial x}\left[kA_{45}\left(\theta_y + \frac{\partial w}{\partial y}\right) + kA_{55}\left(\theta_x + \frac{\partial w}{\partial x}\right)\right] + \\ \frac{\partial}{\partial y}\left[kA_{44}\left(\theta_y + \frac{\partial w}{\partial y}\right) + kA_{45}\left(\theta_x + \frac{\partial w}{\partial x}\right)\right] + q = I_0\frac{\partial^2 w}{\partial t^2}, \quad (36)$$

where $w = w(x, y, t)$ is the transverse displacement, $\theta_x = \theta_x(x, y, t)$ and $\theta_y = \theta_y(x, y, t)$ are the rotations about the x and y axis, respectively, $K = 5/6$ is the shear correction coefficient, and q is the total transverse load.

The initial conditions are the static solution of bending equilibrium. A mesh of 81 points was used, corresponding to 9 equally spaced points per side, in [-1,1], and $\Delta t = 10^{-5}$. The RBF used was the Matérn Cubic (see (12)) and the optimal RBF shape parameter obtained was $\epsilon = 0.104817$.

In figure 2 we present the transverse displacement of the central point of the plate considered along the time $t \in [0, 1]$.

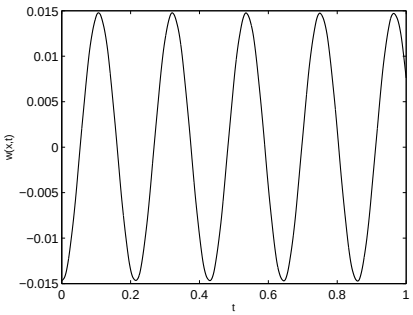

Figure 1. Central displacement of the beam

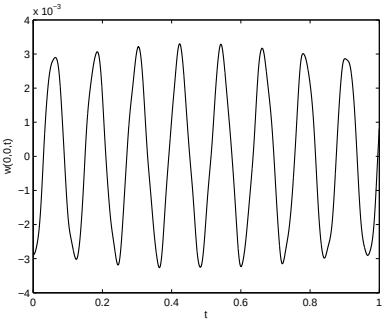

Figure 2. Central displacement of the plate

4. Conclusions

This paper addresses the solution of several PDE problems using a technique that combines the radial basis function (RBF) collocation technique and the pseudospectal (PS) method with the optimization of the RBF shape parameter. This allows the extension of the accurate results to complex geometries, keeping it simple to implement.

Several numerical tests were performed using some radial basis functions, boundary conditions, and initial conditions, for both one and two-dimensional problems. We extended previous work to the transient analysis of a beam and a plate.

Results obtained demonstrate that the method produces good results which are in good agreement with exact solutions or references considered.

Further studies, including the application of the method to composite structures and with more complex geometries are to be made.

References

[1] Trefethen L N 2000 *Spectral Methods in Matlab* (Philadelphia: SIAM)
[2] Fornberg B 1998 *A Practical Guide to Pseudospectral Methods* (Cambridge: Cambridge University Press)
[3] Kansa E J 1990 *Computers & mathematics with applications*, **19(8-9)** 127–145
[4] Kansa E J 1990 *Computers & mathematics with applications*, **19(8-9)** 147–161
[5] Larsson E and Fornberg B 2003 *Computers & Mathematics with Applications*, **46 (5-6)** 891–902
[6] Fasshauer G E 1997 *Proc. of the 3rd Int. Conf. on Curves and Surfaces* **2** 131–138
[7] Sarra S A 2005 *Applied Numerical Mathematics* **54 (11)** 79–94.
[8] Ferreira A J M, Martins P A L S and Roque C M C 2005 *Journal of Sound and Vibration* **280** 595–610
[9] Ferreira A J M and Fasshauer G E 2007 *Composite Structures* **79** 202–210
[10] Ferreira A J M and Fasshauer G E 2006 *Computer Methods in Applied Mechanics and Engineering* **196** 134–146
[11] Fasshauer G E 2005 *Boundary Elements XXVII* 47–56
[12] Ferreira A J M and Fasshauer G E 2007 *Advances in Meshfree Techniques* 283–310
[13] Ferreira A J M, Fasshauer G E, Batra R C and Rodrigues J D 2008 *Composite Structures* **86** 328–343
[14] Fasshauer G E 2007 *Meshfree Approximation Methods with Matlab* (Singapore: World Scientific Publishers)
[15] Reddy J N 1997 *Mechanics of laminated composite plates* (New York: CRC Press)